ORNL/TM-9147
Dist. Category UC-20 g

ORNL/TM--9147

DE84 010636

Fusion Energy Division

EQUILIBRIUM CALCULATIONS FOR HELICAL AXIS STELLARATORS

T. C. Hender
B. A. Carreras

DISCLAIMER

Date Published - April 1984

Prepared by the
Oak Ridge National Laboratory
Oak Ridge, Tennessee 37831
operated by
Martin Marietta Energy Systems, Inc.
for the
U.S. DEPARTMENT OF ENERGY
under Contract No. DE-AC05-840R21400

CONTENTS

ABSTRACT

An average method based on a vacuum flux coordinate system is presented. This average method permits the study of helical axis stellarators with toroidally dominated shifts. An ordering is introduced, and to lowest order the toroidally averaged equilibrium equations are reduced to a Grad-Shafranov equation. Also, to lowest order, a Poisson-type equation is obtained for the toroidally varying corrections to the equilibrium. By including these corrections, systems that are toroidally dominated, but with significant helical distortion to the equilibrium, may be studied. Numerical solutions of the average method equations are shown to agree well with three-dimensional calculations.

1. INTRODUCTION

Studies of the magnetohydrodynamic (MHD) properties of stellarator-type configurations are complicated by the fully three-dimensional (3-D) nature of the device. The study of stellarator equilibria may be reduced, for certain classes of configurations, to a two-dimensional (2-D) problem by the method of averaging.[1] This method was first applied to the calculation of stellarator equilibria by Greene and Johnson.[2] The average method relies on the separation between a toroidally slowly varying magnetic field, dominated by a toroidal component B_T and a rapidly varying helical component $\tilde{\vec{B}}_v$, due to the external helical coils, where the ratio $|\tilde{\vec{B}}_v|/B_T \sim \delta$ is assumed small. Greene and Johnson expanded the equilibrium equations in powers of the inverse aspect ratio ϵ, about the cylindrical limit, to obtain an equilibrium solution. Several variations of this basic technique have been developed. Kovrizhnykh and Shchepetov[3] average the MHD equations directly without recourse to an inverse aspect ratio expansion. Alternatively, Mikhailov[4] solves an inverse equilibrium problem by considering the finite beta deformations to an analytically obtained straight-field-line vacuum coordinate system. Pustovitov[5] has extended this method to an $\ell = 2$ system with a helical axis. All these methods result in equivalent equations for the equilibrium magnetic axis shift.

Recent computational solutions of the averaged equilibrium equations have proven a powerful tool in analyzing stellarator configurations, even for relatively small aspect ratio devices.[6] Comparisons of these average method solutions with those of fully 3-D equilibrium calculations show very good agreement, thus validating the average method.[6] Another benefit of using the average method is that the stability of equilibria obtained can be analyzed by using extensions of the numerical methods used for tokamak stability studies.[6,7,8]

In this paper, an averaging method suitable for studying the equilibrium properties of planar and helical axis systems will be described. The method, based on a straight-field-line vacuum coordinate system, is similar to the averaged equilibrium method described by Pustovitov. In the present paper, however, not only will the averaged equilibria be calculated, but also to leading order the helical corrections will be calculated. The equilibrium equations are averaged in the flux coordinate toroidal angle, and an ordering that is applicable to systems with toroidally dominated equilibrium shifts is used. Certain systems which although the magnetic axis of the vacuum configuration make large helical excursions, still possess the property of having a dominantly toroidal equilibrium shift. The helical-axis variant of the Advanced Toroidal Facility (ATF)[9] device and small aspect ratio heliacs[10] are examples of such configurations. The ordering used is similar to that of Greene and Johnson and allows the dominant terms of the averaged and toroidally varying components of the equilibrium equations to be determined. To lowest order, the averaged

equilibrium equations yield a Grad-Shafranov-type equation, while the toroidally varying terms of the equilibrium equation may be reduced to a Poisson type equation for the toroidally varying toroidal magnetic field. The Grad-Shafranov equation for the averaged equilibrium is similar to that obtained by Greene and Johnson.[2] The Poisson type equation for the toroidally varying toroidal magnetic field, permits the study of higher order corrections to the equilibrium problem, which have not been examined previously.

This combination of averaged equilibrium solutions and first order helical corrections permits the study of toroidally dominated systems that have appreciable helical distortions. In the other limit that the helical shift dominates, the equilibrium properties may be studied by averaging helically. Thus, only the equilibria of systems with comparable helical and toroidal shifts remain inaccessible by 2-D methods.

Several other approaches for studying the equilibrium properties of helical axis configurations may be used. A variant of the Greene and Johnson ordering, which permits the study of helical axis system has been proposed.[11] Alternatively, Reiman and Boozer have used linear approximations to the toroidal and helical shifts[12] to study the fragility of magnetic surfaces[13] and various other properties of helical axis configurations.[14] Another approach that has been used extensively is that of ignoring toroidal effects and studying the MHD properties in the helically symmetric limit.[15] This technique, which is applicable to large aspect ratio devices, has been applied to heliac configurations to study their stability properties.[16]

This paper is presented in the following order. The vacuum flux coordinates and details of the averaging will be described in the next section. In Sec. 3 the results of averaging in the real toroidal angle and the averaging method used here will be compared and contrasted. The equivalence of the two methods will be demonstrated by comparing the expressions for magnetic well and plasma equilibrium shift given by the two methods. Numerical results for the planar and helical axis ATF device are given in Sec. 4. The average method results are shown to agree well with 3-D computations. Conclusions are drawn in Sec. 5.

2 EQUILIBRIUM EQUATIONS FOR THE AVERAGED AND RAPIDLY VARYING QUANTITIES

In this section, the reduction of the magnetohydrodynamic (MHD) equilibrium equations

$$\vec{\nabla}P = \vec{J} \times \vec{B} ,$$
$$\vec{\nabla} \cdot \vec{B} = 0 , \qquad (1)$$

and

$$\vec{\nabla} \times \vec{B} = \vec{J}$$

to equations for the averaged and toroidally varying equilibrium quantities will be described. To facilitate this, an ordering is introduced and, to lowest order, a Grad-Shafranov-type equation is derived from the toroidally averaged equilibrium equations. A Poisson type equation for the toroidally varying components of the equilibrium is also derived. First, however, the vacuum flux coordinates used in the derivations will be described.

2.1 VACUUM FLUX COORDINATES

The vacuum flux coordinates used are those detailed by Boozer.[17] Any vacuum magnetic field may be represented either in contravariant form as

$$\vec{B}_v = B_0 \rho_v \vec{\nabla}\rho_v \times \vec{\nabla}(\theta_v - \iota_v \phi_v) \qquad (2)$$

or in covariant form as

$$\vec{B}_v = F_v \vec{\nabla}\phi_v \ , \tag{3}$$

where $\iota_v(\rho_v)$ is the vacuum rotational transform and F_v is a constant. Here $B_0\rho_v^2/2 \equiv \psi_T$ is the toroidal flux, and ρ_v may be regarded as a radial-like coordinate. The potential ϕ_v takes the role of a toroidal coordinate and for appropriate choice of the constant F_v, changes by 2π in traversing the torus once toroidally. Finally, θ_v is a generalized poloidal angle and changes by 2π in going once around the torus poloidally. These coordinates may be generated numerically in a manner described in Ref. 18, using a modified version of a code developed at Oak Ridge National Laboratory (ORNL). This code generates the Fourier series representation of the standard cylindrical coordinates (R,Z,ς) by following vacuum magnetic field lines. For example, the Fourier representation of R is

$$R(\rho_v,\theta_v,\phi_v) = \sum_{m,n} R_{m,n}(\rho_v) \cos(m\theta_v + n\phi_v) \ . \tag{4}$$

Using these Fourier representations, the necessary metric elements may be generated. In practice, the quasi-cylindrical-like set of coordinates $(\rho_v,(\rho_v\theta_v),\phi_v)$, which have the usual near-axis behavior of the field components is used. The Jacobian is

$$D_v = [\vec{\nabla}\rho_v \times \vec{\nabla}(\rho_v\theta_v)] \cdot \vec{\nabla}\phi_v = \frac{|\vec{B}_v|^2}{B_0 F_v} \ . \tag{5}$$

The ordering of the metric elements and various magnetic field components will now be discussed.

2.2 ORDERING

We may write any quantity in terms of its averaged and rapidly varying parts in ϕ_v:

$$A = \langle A \rangle + \tilde{A} , \tag{6}$$

where

$$\langle A \rangle = \frac{1}{2\pi} \int_0^{2\pi} A \, d\phi_v . \tag{7}$$

In general, $\tilde{A}$ is a periodic function of $M\phi_v$, where M is the number of field periods and is assumed to be $M >> 1$.

From Eqs. (2) and (3) the components of the vacuum magnetic field are

$$B_v^{\rho} = 0 , \tag{8}$$

$$B_v^{\theta} = B_0 \rho_v \varkappa_v D_v , \tag{9}$$

and

$$B_v^{\phi} = B_0 D_v . \tag{10}$$

Examining these equations shows that the natural way of decomposing the magnetic field is:

$$\frac{B^i}{D_v} = \left\langle \frac{B^i}{D_v} \right\rangle + \widetilde{\left(\frac{B^i}{D_v} \right)} ,$$

where $i = \rho_v, \theta_v, \phi_v$.

The ordering of these components is taken to be

$$\left\langle \frac{B^\theta}{D_v} \right\rangle \sim \epsilon \ , \quad \left\langle \frac{B^\phi}{D_v} \right\rangle \sim 1 \ , \text{and} \ \left\langle \frac{B^\rho}{D_v} \right\rangle \sim \beta \sim \epsilon \ , \qquad (11)$$

where it is assumed that $\beta \sim \epsilon$. The ordering of the θ_v and ϕ_v components is compatible with Eqs. (9) and (10), while the ordering of the ρ_v component arises because the B^ρ component is induced by finite beta and toroidal curvature effects. In applying this ordering to the equilibrium equations, we will see that a consistent solution results.

In the vacuum flux coordinate system, the order of the rapidly varying component of the magnetic field is introduced by ordering the metric elements. This is equivalent in real space to assuming an order for the vacuum helical field relative to the toroidal field. The assumption is that

$$\widetilde{(\bar{g}^{\rho\rho})} \sim \widetilde{(\bar{g}^{\theta\theta})} \sim \widetilde{(\bar{g}^{\rho\theta})} \sim \widetilde{(\bar{g}^{\phi\phi})} \sim \delta \ , \qquad (12)$$

where the relation $\epsilon \sim \delta^2$ is assumed and the number of field periods $M \sim \epsilon^{-1}$. These orderings, together with the assumption that the equilibrium shift is toroidally dominated, permit the orderings of the remaining quantities to be determined. For example we find,

$$\widetilde{\left(\frac{B^{\rho}}{D_v}\right)} \sim \widetilde{\left(\frac{B^{\theta}}{D_v}\right)} \sim \epsilon\delta \ . \tag{13}$$

Physically, this ordering arises because the fluctuating terms are generated, as finite-beta effects, by the beating of the toroidal shift (order β) with fluctuating metric elements (order δ). Some care must be taken in interpreting the consequences of this ordering on the magnetic axis shift. The helical iota bar that governs the shift caused by the helical harmonics is $\iota_h = M - \iota_v$. Thus, a configuration with a low ι/M may have a toroidally dominated shift but may violate the ordering by having $\widetilde{(B^i/D_v)}$ larger than $\langle B^i/D_v \rangle$.

The ordering given above is basically that of Greene and Johnson.[2] However, by working in a vacuum flux coordinate system, certain important differences arise. Some insight may be gained by examining the equilibrium relation $\vec{B} \cdot \vec{\nabla}P = 0$. This relation may be split into its averaged and rapidly varying parts:

$$\langle\vec{B}\rangle \cdot \vec{\nabla}\langle P\rangle + \langle\tilde{\vec{B}} \cdot \vec{\nabla}\tilde{P}\rangle = 0 \tag{14}$$

and

$$\tilde{\vec{B}} \cdot \vec{\nabla}\langle P\rangle + \langle\vec{B}\rangle \cdot \vec{\nabla}\tilde{P} = 0 \ . \tag{15}$$

From the ordering used, Eq. (15) shows that $\tilde{P} \sim \delta^5$. Hence,

$$\frac{\langle\tilde{\vec{B}} \cdot \vec{\nabla}\tilde{P}\rangle}{\langle\vec{B}\rangle \cdot \vec{\nabla}\langle P\rangle} \sim \delta^4 \ , \tag{16}$$

averaging in real toroidal angle $\tilde{\vec{B}} = \tilde{\vec{B}}_v \sim \delta$ and $\tilde{P} \sim \delta^3$, and therefore the ratio in Eq. (16) is of order unity. Thus, the quasi-linear term $\langle \tilde{\vec{B}} \cdot \vec{\nabla}\tilde{P} \rangle$ must be explicitly retained in the equilibrium equation when averaging in real space. However, by averaging over ϕ_v at fixed ρ_v, θ_v these corrections are implicitly retained. Therefore, in the vacuum flux coordinate system, the magnetic field associated with the averaged pressure (or flux) surfaces is the averaged magnetic field. Averaging in real toroidal angle, it is necessary to introduce an effective magnetic field that takes into account the quasi-linear contributions from rapidly varying terms. This will be discussed in greater detail in Sec. 3.

Having established these orderings, it is now possible to derive a Grad-Shafranov-type equation from the averaged equilibrium equations and an equation for the toroidally varying components of the equilibrium.

2.3 AVERAGED EQUILIBRIUM EQUATIONS

To leading order, the toroidally averaged radial component of the equilibrium equation ($\vec{\nabla}P = \vec{J} \times \vec{B}$) is

$$-\left\langle \frac{B^\phi}{D_v} \right\rangle \frac{\partial}{\partial \rho_v} \langle B_\phi \rangle - \left\langle \frac{B^\theta}{D_v} \right\rangle \left[\frac{1}{\rho_v} \frac{\partial}{\partial \rho_v} (\rho_v \langle B_\theta \rangle) - \frac{1}{\rho_v} \frac{\partial}{\partial \theta_v} \langle B_\rho \rangle \right] = \left\langle \frac{1}{D_v} \right\rangle \frac{\partial \langle P \rangle}{\partial \rho_v} . \tag{17}$$

As mentioned in the previous section, corrections to this equation

arising from quasi-linear products of fluctuating terms need not be retained because they are of higher order.

The θ_v and ϕ_v components of the averaged equilibrium equation yield to leading order

$$\left\langle \frac{B^\rho}{D_v} \right\rangle \left[\frac{1}{\rho_v} \frac{\partial}{\partial \rho_v} (\rho_v \langle B_\theta \rangle) - \frac{1}{\rho_v} \frac{\partial}{\partial \theta_v} \langle B_\rho \rangle \right] - \left\langle \frac{B^\phi}{D_v} \right\rangle \frac{1}{\rho_v} \frac{\partial \langle B_\phi \rangle}{\partial \theta_v} = \left\langle \frac{1}{D_v} \right\rangle \frac{1}{\rho_v} \frac{\partial \langle P \rangle}{\partial \theta_v} \tag{18}$$

and

$$\left\langle \frac{B^\theta}{D_v} \right\rangle \frac{1}{\rho_v} \frac{\partial \langle B_\phi \rangle}{\partial \theta_v} + \left\langle \frac{B^\rho}{D_v} \right\rangle \frac{\partial \langle B_\phi \rangle}{\partial \rho_v} = 0 \, . \tag{19}$$

From $\langle \vec{\nabla} \cdot \vec{B} \rangle = 0$, an averaged poloidal flux function ψ may be defined by

$$\left\langle \frac{B^\rho}{D_v} \right\rangle = \frac{1}{\rho_v} \frac{\partial \psi}{\partial \theta_v} \quad \text{and} \quad \left\langle \frac{B^\theta}{\Gamma_v} \right\rangle = - \frac{\partial \psi}{\partial \rho_v} \, . \tag{20}$$

Note that in limit $\beta = 0$,

$$\psi = \int_0^\rho \rho_v d\rho_v \iota_v(\rho_v) \tag{21}$$

is the vacuum poloidal flux function (ψ_v). Equations (19) and (20) show that $\langle B_\phi \rangle$ is a function ψ alone. Also, since $\langle \vec{B} \rangle \cdot \vec{\nabla} \langle P \rangle = 0$, $\langle P \rangle$ is a function of ψ only. Thus, Eqs. (17) and (18) are equivalent to

$$\frac{1}{\rho_v}\frac{\partial}{\partial\rho_v}(\rho_v\langle B_\theta\rangle) - \frac{1}{\rho_v}\frac{\partial}{\partial\theta_v}\langle B_\rho\rangle = \left\langle\frac{B^\phi}{D_v}\right\rangle\frac{dF}{d\psi} + \left\langle\frac{1}{D_v}\right\rangle\frac{d\langle P\rangle}{d\psi}, \quad (22)$$

where $F(\psi) \equiv \langle B_\phi\rangle$ and for $\beta = 0$, $F(\psi_v) = F_v$. This equation may be cast into a more familiar form by use of various properties of the metric elements. The following relationships between the covariant and contravariant components occur:

$$\langle B_\rho\rangle = \frac{B_0}{F_v\alpha_v}\left(\langle\bar{g}^{\theta\theta}\rangle\frac{1}{\rho_v}\frac{\partial\psi}{\partial\theta_v} + \langle\bar{g}^{\rho\theta}\rangle\frac{\partial\psi}{\partial\rho_v} + \frac{B_0\rho_v}{F_v}\tau_v F\langle\bar{g}^{\rho\theta}\rangle\right),$$

$$\langle B_\theta\rangle = \frac{B_0}{F_v\alpha_v}\left(-\langle\bar{g}^{\rho\theta}\rangle\frac{1}{\rho_v}\frac{\partial\psi}{\partial\theta_v} - \langle\bar{g}^{\rho\rho}\rangle\frac{\partial\psi}{\partial\rho_v} - \frac{B_0\rho_v}{F_v}\tau_v F\langle\bar{g}^{\rho\rho}\rangle\right), \quad (23)$$

and

$$\left\langle\frac{B^\phi}{D_v}\right\rangle = \frac{B_0}{F_v\alpha_v}\left[F - \frac{\rho_v B_0}{F_v}\tau_v\left(\frac{\langle\bar{g}^{\rho\theta}\rangle}{\rho_v}\frac{\partial\psi}{\partial\theta_v} + \langle\bar{g}^{\rho\rho}\rangle\frac{\partial\psi}{\partial\rho_v}\right)\right] \quad (24)$$

where $\alpha_v = 1 + \frac{B_0^2\rho_v^2}{F_v^2}\tau_v^2\langle\bar{g}^{\rho\rho}\rangle$. Substituting Eqs. (23) and (24) into Eq. (22) yields to leading order, a Grad-Shafranov type equation

$$\frac{1}{\rho_v}\frac{\partial}{\partial\rho_v}\left(\rho_v\langle\bar{g}^{\rho\rho}\rangle\frac{\partial\psi}{\partial\rho_v} + \langle\bar{g}^{\rho\theta}\rangle\frac{\partial\psi}{\partial\theta_v}\right) + \frac{1}{\rho_v}\frac{\partial}{\partial\theta_v}\left(\langle\bar{g}^{\rho\theta}\rangle\frac{\partial\psi}{\partial\rho_v} + \frac{\langle\bar{g}^{\theta\theta}\rangle}{\rho_v}\frac{\partial\psi}{\partial\theta_v}\right)$$

$$+ \frac{B_0F}{F_v}\left[\frac{1}{\rho_v}\frac{\partial}{\partial\rho_v}(\rho_v^2\tau_v\langle\bar{g}^{\rho\rho}\rangle) + \frac{1}{\rho_v}\frac{\partial}{\partial\theta_v}(\rho_v\tau_v\langle\bar{g}^{\rho\theta}\rangle)\right]$$

$$= \frac{-F_v}{B_0} \left\langle \frac{1}{D_v} \right\rangle \frac{dP}{d\psi} - F\frac{dF}{d\psi} . \qquad (25)$$

As will be discussed in Sec. 3, this equation is equivalent to that obtained by Greene and Johnson. However, by averaging in flux coordinates, the vacuum quantities enter in a simple and natural manner.

2.4 TOROIDALLY VARYING CORRECTIONS

Equation (25) was obtained by retaining the leading-order terms of the toroidally averaged equilibrium equation. By retaining the leading-order terms of the toroidally varying parts of the equilibrium equations, we obtain helical corrections to the equilibrium. As mentioned above, the quasi-linear contributions from these helical terms to the averaged equations are of higher order and need not be retained. However, for configurations with dominantly toroidal shift, but with significant helical distortions, such corrections may still be important.

To leading order, the toroidally varying radial and poloidal projections of $\vec{\nabla}P = \vec{J} \times \vec{B}$ are

$$\frac{\partial \tilde{B}_\rho}{\partial \phi_v} = \frac{\partial \tilde{B}_\phi}{\partial \rho_v} + \widetilde{\left(\frac{1}{D_v}\right)} \frac{\partial \langle P \rangle}{\partial \rho_v} \left\langle \frac{B^\phi}{D_v} \right\rangle^{-1} \qquad (26)$$

and

$$\frac{\partial \tilde{B}_\theta}{\partial \phi_v} = \frac{1}{\rho_v}\frac{\partial \tilde{B}_\phi}{\partial \theta_v} + \left(\widetilde{\frac{1}{D_v}}\right)\frac{1}{\rho_v}\frac{\partial \langle P\rangle}{\partial \theta_v}\left\langle \frac{B^\phi}{D_v}\right\rangle^{-1} , \tag{27}$$

and the fluctuating component of $\vec{\nabla} \cdot \vec{B} = 0$ is

$$\frac{1}{\rho_v}\frac{\partial}{\partial \rho_v}\left[\rho_v\left(\widetilde{\frac{B^\rho}{D_v}}\right)\right] + \frac{1}{\rho_v}\frac{\partial}{\partial \theta_v}\left(\widetilde{\frac{B^\theta}{D_v}}\right) + \frac{\partial}{\partial \phi_v}\left(\widetilde{\frac{B^\phi}{D_v}}\right) = 0 . \tag{28}$$

These three equations determine, with proper boundary conditions, the three rapidly varying components of the magnetic field. A fourth, independent equation may be obtained from the leading-order terms of Eq. (15) for $\tilde{P}$:

$$\left\langle \frac{B^\phi}{D_v}\right\rangle \frac{\partial \tilde{P}}{\partial \phi_v} = -\left(\widetilde{\frac{B^\rho}{D_v}}\right)\frac{\partial \langle P\rangle}{\partial \rho_v} - \left(\widetilde{\frac{B^\theta}{D_v}}\right)\frac{1}{\rho_v}\frac{\partial \langle P\rangle}{\partial \theta_v} . \tag{29}$$

Equations (26) through (28) may be combined into a single equation for $\tilde{B}_\phi$ by using the relationships between the covariant and contravariant components of the magnetic field:

$$\begin{aligned}
\left(\widetilde{\frac{B^\rho}{D_v}}\right) &= \left\langle \frac{g^{\rho\rho}}{D_v}\right\rangle \tilde{B}_\rho + \left\langle \frac{g^{\rho\theta}}{D_v}\right\rangle \tilde{B}_\theta + \tilde{b}_\rho , \\
\left(\widetilde{\frac{B^\theta}{D_v}}\right) &= \left\langle \frac{g^{\rho\theta}}{D_v}\right\rangle \tilde{B}_\rho + \left\langle \frac{g^{\theta\theta}}{D_v}\right\rangle \tilde{B}_\theta + \tilde{b}_\theta , \\
\left(\widetilde{\frac{B^\phi}{D_v}}\right) &= \frac{B_0}{F_v}\tilde{B}_\phi ,
\end{aligned} \tag{30}$$

where only leading order terms are retained and

$$\tilde{b}_\rho = \widetilde{(\bar{g}^{\rho\rho})} \frac{1}{\rho_v} \frac{\partial \psi}{\partial \theta_v} - \widetilde{(\bar{g}^{\rho\theta})} \frac{\partial \psi}{\partial \rho_v} ,$$

$$\tilde{b}_\theta = \widetilde{(\bar{g}^{\rho\theta})} \frac{1}{\rho_v} \frac{\partial \psi}{\partial \theta_v} - \widetilde{(\bar{g}^{\theta\theta})} \frac{\partial \psi}{\partial \rho_v} . \qquad (31)$$

When the averaged equilibrium equation [Eq. (25)] is solved, $\tilde{b}_\rho$ and $\tilde{b}_\theta$ are fully determined. By substituting Eqs. (26) and (27) into Eqs. (30), relations for $\widetilde{(B^\rho/D_v)}$ and $\widetilde{(B^\theta/D_v)}$ in terms of $\tilde{B}_\phi$, $\tilde{b}_\rho$, and $\tilde{b}_\theta$ may be obtained. These relations may then be substituted into Eq. (28) to yield:

$$\frac{1}{\rho_v} \frac{\partial}{\partial \rho_v} \left[\rho_v \left(\left\langle \frac{\bar{g}^{\rho\rho}}{D_v} \right\rangle \frac{\partial \tilde{B}_\phi}{\partial \rho_v} + \frac{1}{\rho_v} \left\langle \frac{\bar{g}^{\rho\theta}}{D_v} \right\rangle \frac{\partial \tilde{B}_\phi}{\partial \theta_v} \right) \right]$$

$$+ \frac{1}{\rho_v} \frac{\partial}{\partial \theta_v} \left(\left\langle \frac{\bar{g}^{\rho\theta}}{D_v} \right\rangle \frac{\partial \tilde{B}_\phi}{\partial \rho_v} + \frac{1}{\rho_v} \left\langle \frac{\bar{g}^{\theta\theta}}{D_v} \right\rangle \frac{\partial \tilde{B}_\phi}{\partial \theta_v} \right)$$

$$+ \frac{B_0}{F_v} \frac{\partial^2 \tilde{B}_\phi}{\partial \phi_v^2} = \frac{-1}{\rho_v} \frac{\partial}{\partial \rho_v} \left\{ \rho_v \left[\left\langle \frac{\bar{g}^{\rho\rho}}{D_v} \right\rangle \tilde{P}_\rho + \left\langle \frac{\bar{g}^{\rho\theta}}{D_v} \right\rangle \tilde{P}_\theta - \frac{\partial}{\partial \phi_v} \left(\left\langle \frac{\bar{g}^{\rho\rho}}{D_v} \right\rangle \tilde{b}_\rho \right) \right.\right.$$

$$\left.\left. - \frac{\partial}{\partial \phi_v} \left(\left\langle \frac{\bar{g}^{\rho\theta}}{D_v} \right\rangle \tilde{b}_\theta \right) \right] \right\} - \frac{1}{\rho_v} \frac{\partial}{\partial \theta_v} \left[\left\langle \frac{\bar{g}^{\rho\theta}}{D_v} \right\rangle \tilde{P}_\rho + \left\langle \frac{\bar{g}^{\theta\theta}}{D_v} \right\rangle \tilde{P}_\theta \right.$$

$$\left. - \frac{\partial}{\partial \phi_v} \left(\left\langle \frac{\bar{g}^{\rho\theta}}{D_v} \right\rangle \tilde{b}_\rho \right) - \frac{\partial}{\partial \phi_v} \left(\left\langle \frac{\bar{g}^{\theta\theta}}{D_v} \right\rangle \tilde{b}_\theta \right) \right] \qquad (32)$$

where

$$\tilde{P}_\rho = \widetilde{\left(\frac{1}{D_v}\right)} \frac{\partial \langle P \rangle}{\partial \rho_v} \left\langle \frac{B^\phi}{D_v} \right\rangle^{-1} ,$$

$$\tilde{P}_\theta = \widetilde{\left(\frac{1}{D_v}\right)} \frac{1}{\rho_v} \frac{\partial \langle P \rangle}{\partial \theta_v} \left\langle \frac{B^\phi}{D_v} \right\rangle^{-1} .$$

The right-hand side of Eq. (32) is fully determined when the averaged equilibrium equation [Eq. (25)] has been solved. Hence, $\tilde{B}_\phi$ may be determined, and the other fluctuating quantities ($\tilde{B}_\rho$,$\tilde{B}_\theta$) may in turn be found. This procedure has been numerically implemented, and the results will be described in Sec. 4. Therefore, the solution of the 3-D equilibrium problem has been reduced to solving the 2-D equations, Eqs. (25) and (32).

3. COMPARISON WITH THE REAL SPACE AVERAGE METHOD

In this section we will establish the equivalence of averaging in real toroidal angle and averaging in the vacuum flux coordinates of this paper. To achieve this we will examine the Grad-Shafranov equation [Eq. (25)] and identify its terms with those of the average method Grad-Shafranov equation derived by Greene and Johnson. We will also very briefly sketch the derivation of an equilibrium shift equation from Eq. (25) and show that it too is equivalent to the shift equation obtained in Ref. 19.

In the vacuum flux coordinates the derivative of the vacuum volume (V_v) with respect to vacuum toroidal flux (ψ_{Tv}) is

$$V_v' = \frac{dV_v}{d\psi_{Tv}} = \frac{1}{B_0} \int_0^{2\pi} \left\langle \frac{1}{D_v} \right\rangle d\theta_v \ , \tag{33}$$

where the integral is to be evaluated at constant ρ_v. Writing

$$\vec{B}_v = F_v(\vec{\nabla}\phi + \delta\vec{\nabla}\tilde{\phi}_v) \ , \tag{34}$$

then to order δ^2, Eq. (33) becomes

$$V_v' = \frac{1}{F_v} \int_0^{2\pi} d\theta_v \left(R^2 - 2\delta R_0^4 \langle \vec{\nabla}\phi \cdot \vec{\nabla}\tilde{\phi}_v \rangle - \delta^2 R_0^4 \langle |\vec{\nabla}\tilde{\phi}|^2 \rangle\right) \ . \tag{35}$$

This equation appears to have the opposite sign for the helical contributions to the well (third term in the integral), compared to the Greene and Johnson expression. However, the averages over ϕ_v in

Eq. (35) are at constant ρ_v and θ_v; taking this into account, the second term in the integral is nonzero and is such that $\langle \vec{\nabla} \tilde{\vec{\nabla}} \tilde{\phi} \rangle \simeq -\delta \langle |\tilde{\vec{\nabla}} \tilde{\phi}|^2 \rangle$, cancelling the contribution from the third term and resolving the apparent contradiction.

Defining

$$\nabla_\perp^2 \equiv \frac{1}{\rho_v} \frac{\partial}{\partial \rho_v} \left(\rho_v \langle \bar{g}^{\rho\rho} \rangle \frac{\partial}{\partial \rho_v} + \langle \bar{g}^{\rho\theta} \rangle \frac{\partial}{\partial \theta_v} \right) + \frac{1}{\rho_v} \frac{\partial}{\partial \theta_v} \left(\langle \bar{g}^{\rho\theta} \rangle \frac{\partial}{\partial \rho_v} + \frac{\langle \bar{g}^{\theta\theta} \rangle}{\rho_v} \frac{\partial}{\partial \theta_v} \right)$$

and noting that the vacuum ψ is given by

$$\frac{d\psi_v}{d\rho_v} = -B_0 \iota_v \rho_v \ ,$$

we may rewrite to leading order the Grad-Shafranov equation [Eq. (25)] as

$$\nabla_\perp^2 (\psi - \psi_v) = -\left(R^2 - 2\delta R_0^4 \langle \vec{\nabla}\phi \cdot \tilde{\vec{\nabla}} \tilde{\phi}_v \rangle - \delta^2 R_0^4 \langle |\tilde{\vec{\nabla}} \tilde{\phi}|^2 \rangle \right) \frac{d\langle P \rangle}{d\psi} - F \frac{dF}{d\psi} \ . \tag{36}$$

Therefore, Eq. (25) may be cast in a form similar to that given by Greene and Johnson[2] and by Strauss.[20]

The derivation of the equilibrium shift equation, from Eq. (25), is in two distinct stages. First, Eq. (25) is transformed into equilibrium flux coordinates (ρ,θ,ϕ_v) defined by

$$\vec{B} = B_0 \rho \vec{\nabla}\rho \times \vec{\nabla}(\theta - \iota \phi_v) \ . \tag{37}$$

The metric elements in these coordinates are related to those of the vacuum coordinates, for example:

$$g^{\rho\rho} = \left(\frac{\partial\rho}{\partial\rho_v}\right)^2 \bar{g}^{\rho\rho} + \frac{2}{\rho_v}\frac{\partial\rho}{\partial\rho_v}\frac{\partial\rho}{\partial\theta_v}\bar{g}^{\rho\theta} + \frac{1}{\rho_v{}^2}\left(\frac{\partial\rho}{\partial\theta_v}\right)^2 \bar{g}^{\theta\theta} \ . \tag{38}$$

The second stage of the derivation is to approximate the flux coordinates analytically. Particularizing to an $\ell = 2$ single helicity system and making a near-axis expansion, the vacuum flux coordinates are

$$\rho_v{}^2 = \hat{r}^2\left(1 - \delta_1 \cos 2\hat{\theta}_h\right) \ ,$$

$$\theta_v = \hat{\theta} + \frac{\delta_1}{2} \sin 2\hat{\theta}_h \ , \tag{39}$$

and

$$\phi_v = \hat{\phi} + \frac{\delta_1}{2M}\left(\frac{M\hat{r}}{R_0}\right)^2 \sin 2\hat{\theta}_h \ ,$$

where δ_1 is the ratio of the helical to toroidal field, M is the number of field periods, $(\hat{r},\hat{\theta},\hat{\phi})$ are normal cylindrical coordinates, and

$\hat{\theta}_h = \hat{\theta} - M\hat{\phi}$. From Eqs. (39) we may obtain expressions for the vacuum metric elements. Then, relating the vacuum and equilibrium coordinates by a shifted circle model,

$$\rho_v \cos \theta_v = a_0 + \rho \cos \theta + a_2 \cos 2\theta$$

and

(40)

$$\rho_v \sin \theta_v = \rho \sin \theta + a_2 \sin 2\theta \ ,$$

where the shift is $\Delta_p = a_0 + a_2$; and using relations between the equilibrium and vacuum flux coordinates [e.g., Eq. (38)] yields analytic forms for the equilibrium flux coordinate metric elements. Substituting these into the equilibrium coordinate form of the Grad-Shafranov equation yields:

$$\frac{1}{\rho^2 \tau} \frac{d}{d\rho} \left(\rho^3 \tau^2 \frac{d\Delta_p}{d\rho} \right) + \frac{\Delta_p}{\rho^2} \frac{d}{d\rho} \left(\rho^3 \frac{d\tau}{d\rho} \right) = \frac{1}{\tau} \left(\frac{R_0}{B_0} + \Delta_p V_v'' \right) \frac{d\langle P \rangle}{d\rho} \ , \qquad (41)$$

where for the particular analytic example of an $\ell = 2$ single helicity system, the well is

$$V_v'' = \frac{2\delta_1^2 M^2}{R_0^2 B_0^2} \ .$$

This form of the equilibrium shift equation [Eq. (41)] is precisely that given by Greene, Johnson, and Weimer.[19]

4. NUMERICAL RESULTS

In this section, the results from numerically solving the Grad-Shafranov equation [Eq. (25)] and the equation for the helical corrections [Eq. (32)] will be compared with those from 3-D computations using the NEAR code.[21] The NEAR code is a 3-D equilibrium code that uses the (ρ_v,θ_v,ϕ_v) coordinates as its Eulerian frame of reference and relaxes the equations to an equilibrium by an energy-minimization technique.

Before presenting the results, the numerical methods will be described briefly. The Grad-Shafranov equation [Eq. (25)] is not solved directly as a Poisson type problem; instead, an energy-minimization technique is used to solve the equivalent Eqs. (17) and (18). A fictitious force $\vec{F}$ is introduced:

$$F_\rho = -\left\langle \frac{B^\phi}{D_v} \right\rangle \frac{\partial}{\partial \rho_v} \langle B_\phi \rangle - \left\langle \frac{B^\theta}{D_v} \right\rangle \left[\frac{1}{\rho_v} \frac{\partial}{\partial \rho_v} (\rho_v \langle B_\theta \rangle) - \frac{1}{\rho_v} \frac{\partial \langle B_\rho \rangle}{\partial \theta_v} \right] - \left\langle \frac{1}{D_v} \right\rangle \frac{\partial \langle P \rangle}{\partial \rho_v} \tag{42}$$

and

$$F_\theta = -\left\langle \frac{B^\phi}{D_v} \right\rangle \frac{1}{\rho_v} \frac{\partial \langle B_\phi \rangle}{\partial \theta_v} + \left\langle \frac{B^\rho}{D_v} \right\rangle \left[\frac{1}{\rho_v} \frac{\partial}{\partial \rho_v} (\rho_v \langle B_\theta \rangle) - \frac{1}{\rho_v} \frac{\partial \langle B_\rho \rangle}{\partial \theta_v} \right]$$
$$- \left\langle \frac{1}{D_v} \right\rangle \frac{1}{\rho_v} \frac{\partial \langle P \rangle}{\partial \theta_v} . \tag{43}$$

The poloidal and radial components of $\vec{F}$ are related to a velocity $\vec{V}$, using a conjugate gradient scheme:[22]

$$\vec{V}^{n+1} = \vec{F}^{n+1} + \alpha \frac{(\bar{F}^2)^{n+1}}{(\bar{F}^2)^n} \vec{V}^n \quad . \tag{44}$$

The superscripts denote the iteration step, α is a constant just less than unity, and the bar denotes a volume integral. Here, since we are solving an axisymmetric problem in the vacuum flux surface coordinates $(\partial/\partial\phi_v \equiv 0)$, $F_\phi = 0$ may be assumed since $F_\rho = F_\theta = 0$ implies $F_\phi = 0$. Using the velocity, the magnetic field is advanced in a flux-conserving manner:

$$\frac{\partial \langle \vec{B} \rangle}{\partial t} = \nabla \times (\vec{V} \times \langle \vec{B} \rangle) \; ; \tag{45}$$

and, finally, the pressure is assumed to be a given function of ψ, in particular

$$\langle P \rangle = a\psi^m \; , \tag{46}$$

where a and m are constants. At the wall, flux-conserving boundary conditions are imposed.

The equation for the toroidally varying corrections [Eq. (32)] is solved in a different manner. Since numerically the metric elements ($\bar{g}^{\rho\rho}$, etc.) are represented as Fourier series in the angle variables (θ_v, ϕ_v), Eq. (32) may be reduced to a large set of ordinary differential equations (one per helical mode). This set of ODE's is solved using a library boundary value routine — the wall boundary

condition being that $\tilde{B}^{\rho} = 0$. In practice, only the dominant helicity of the helical windings and two side bands are solved for.

The numerical results will now be presented. First, results will be given for the planar axis ATF configuration. ATF is a 12-field period $\ell = 2$ torsatron with a plasma aspect ratio of 7. Figure 1 shows a comparison between the equilibrium flux surfaces in configuration space $(\rho_v, \theta_v, \phi_v)$ and real space for the ATF device with a peak beta, $\beta_0 = 5\%$. The equilibrium shown in Fig. 1 is calculated using the 3-D NEAR code. The equilibrium appears almost axisymmetric in the flux coordinate space. In Fig. 2, a comparison between the equilibrium flux surfaces ($\beta_0 = 5\%$) computed using the average method and a 3-D calculation is given for the planar axis ATF (the vacuum flux surfaces are also shown for reference). The average method and 3-D calculations agree well. Figure 3 makes this comparison more quantitative by comparing the averaged magnetic axis shift (Δ_ρ) as a function of peak beta between the average and 3-D calculations. Here the shift is defined as the displacement of the magnetic axis in flux coordinate ρ_v, divided by the flux coordinate wall radius.

By imbalancing the currents in the helical windings it is possible to form a helical axis plasma in the ATF device. The relatively low aspect ratio and low iotabar per field period result in the helical axis ATF variant still having a toroidally dominated shift. Figure 4 shows a comparison between the equilibrium flux surfaces ($\beta_0 = 2.6\%$) computed using the average method and those computed by NEAR. Again the vacuum flux surfaces are shown for reference. The shifts (Δ_ρ) as computed with NEAR and the average method, for the helical axis ATF,

are shown in Fig. 5. The average method agrees reasonably well with the 3-D computations — the agreement being best at low beta, where the orderings are most valid. Comparing the shifts of the planar and helical axis ATF configurations shows that the latter has a larger initial rate of shift. This is because the so called critical $\beta_c = (2\iota^2\epsilon)$, which gives a measure of the maximum tolerable beta, is smaller for the helical axis ATF. (ι for the helical axis ATF ($\sim$0.6) is about half that of planar axis configuration) Figure 6 shows a comparison between the V′ profile computed with the 3-D NEAR code and with the average method, for the same equilibrium as shown in Fig. 4. The 3-D and average method are in good agreement.

To quantify the accuracy of the corrections to the averaged equilibrium given by Eq. (32), the dominant, toroidally varying, radial magnetic field component computed by the 3-D code (NEAR) and by solving Eq. (32) will be compared. The radial magnetic field is reconstructed using the identity

$$B^\rho = D_v \left[\frac{1}{\rho_v} \frac{\partial \psi}{\partial \theta_v} + \widetilde{\left(\frac{B^\rho}{D_v} \right)} \right] , \tag{47}$$

where the toroidally varying part is computed by solving Eq. (32). Figure 7 shows a comparison of radial magnetic field structure computed with NEAR (3-D) and from the average method (Eq. (47)) for the helical axis ATF with $\beta_0 = 2\%$. The dominant toroidal harmonic ($m = 1, n = 0$) and helical harmonic ($m = 1, n = 6$) are shown in Fig. 7. To distinguish the importance of the helical correction $\widetilde{(B^\rho/D_v)}$, the radial field for

the (1,6) harmonic is shown with and without this correction (Fig. 7). The effect of the helical correction on the (1,0) harmonic is small. The average method with the toroidally varying correction agrees well with the 3-D result. This comparison was made at $\beta_0 = 2\%$. At higher beta (~10%), as the validity of the ordering assumptions is violated, the accuracy of the helical corrections deteriorates.

6. CONCLUSIONS

An averaging method based on a vacuum flux coordinate system has been described. The toroidally averaged equilibrium equations permit the study of planar and helical axis systems with toroidally dominated shifts. An ordering similar to that of Greene and Johnson is introduced to identify the dominant terms in the equilibrium equations. To lowest order, the toroidally averaged equilibrium equations reduce to a Grad-Shafranov equation. Also, to lowest order, the toroidally varying part of the equilibrium equations may be reduced to a Poisson-type equation for the toroidally varying toroidal field $\tilde{B}_\phi$. Equilibria that are toroidally dominated but which have significant helical distortion may thus be studied with this average method.

Numerical results presented for the planar and helical axis ATF show good agreement between the average method and 3-D calculations of equilibria. For the helical axis ATF, the helical corrections [Eq. (32)] to the average-method equilibria are also shown to be in good agreement with 3-D NEAR results, in the low-beta regime where the ordering assumptions are valid.

REFERENCES

1. N. K. Bogolyubov and Yu. A. Mitropol'skij, Asymptotic Methods in the Theory of Non-Linear Oscillations (Nauka, Moscow, 1974).
2. J. M. Greene and J. L. Johnson, Phys. Fluids 4, 875 (1961).
3. L. M. Kovrizhnykh and S. V. Shchepetov, Sov. J. Plasma Phys. 6, 533 (1980); L. M. Kovrizhnykh and S. V. Shchepetov, Preprint No. 36 (P. N. Lebedev Physics Institute, Academy of Sciences of the U.S.S.R., Moscow, 1980).
4. M. I. Mikhailov, Sov. J. Plasma Phys. 6, 25 (1980).
5. V. D. Pustovitov, Sov. J. Plasma Phys. 8, 265 (1983).
6. B. A. Carreras, H. R. Hicks, J. A. Holmes, V. E. Lynch, L. Garcia, J. H. Harris, T. C. Hender, and B. F. Masden, Phys. Fluids 26, 3569 (1983).
7. G. Anania and J. L. Johnson, Phys. Fluids 26, 3070 (1983).
8. H. R. Strauss and D. A. Monticello, Phys. Fluids 24, 1148 (1981).
9. J. F. Lyon, B. A. Carreras, J. H. Harris, J. A. Rome, R. A. Dory, L. Garcia, T. C. Hender, S. P. Hirshman, T. C. Jernigan, J. Sheffield, L. A. Charlton, R. H. Fowler, H. R. Hicks, J. A. Holmes, V. E. Lynch, B. F. Masden, D. L. Goodman, and S. A. Hokin, Oak Ridge National Laboratory Report No. ORNL/TM-8496, 1983.
10. A. H. Boozer, T. K. Chu, R. L. Dewar, H. P. Furth, J. A. Goree, J. L. Johnson, R. M. Kulsrud, D. A. Monticello, G. Kuo-Petravic, G. V. Sheffield, S. Yoshikawa, and O. Betancourt in Plasma Physics and Controlled Nuclear Fusion Research (IAEA, Vienna, 1983), Vol. 3, p. 129.

11. A. E. Koniges, J. L. Johnson, K. E. Weimer, D. Dobrott, Bull. Am. Phys. Soc. 28, 1183 (1983).

12. A. H. Boozer, Princeton Plasma Physics Laboratory Report PPPL-1973, 1983.

13. A. H. Reiman, A. H. Boozer, Princeton Plasma Physics Laboratory Report PPPL-2082, 1983.

14. A. H. Reiman, A. H. Boozer, Phys. Fluids 26, 3167 (1983).

15. D. Lortz and J. Nuhrenberg, Plasma Physics and Controlled Nuclear Fusion Research (IAEA, Vienna, 1978) Vol. 2, p. 309.

16. D. A. Monticello, R. L. Demar, H. P. Furth and A. H. Reiman, Princeton Plasma Physics Laboratory Report PPPL-2036 1983.

17. A. H. Boozer, Phys. Fluids 25, 520 (1982).

18. G. Kuo-Petravic, A. H. Boozer, J. A. Rome, R. H. Fowler, J. Comp. Phys. 51, 261 (1983).

19. J. M. Greene, J. L. Johnson, and K. E. Weimer, Plasma Phys. 8, 145 (1965).

20. H. R. Strauss, Plasma Phys. 22, 733 (1980).

21. T. C. Hender, B. A. Carreras, V. E. Lynch, J. A. Rome, Bull. Am. Phys. Soc. 27, 1020 (1982).

22. R. Chodura and A. Schlüter, J. Comput. Phys. 41, 68 (1981).

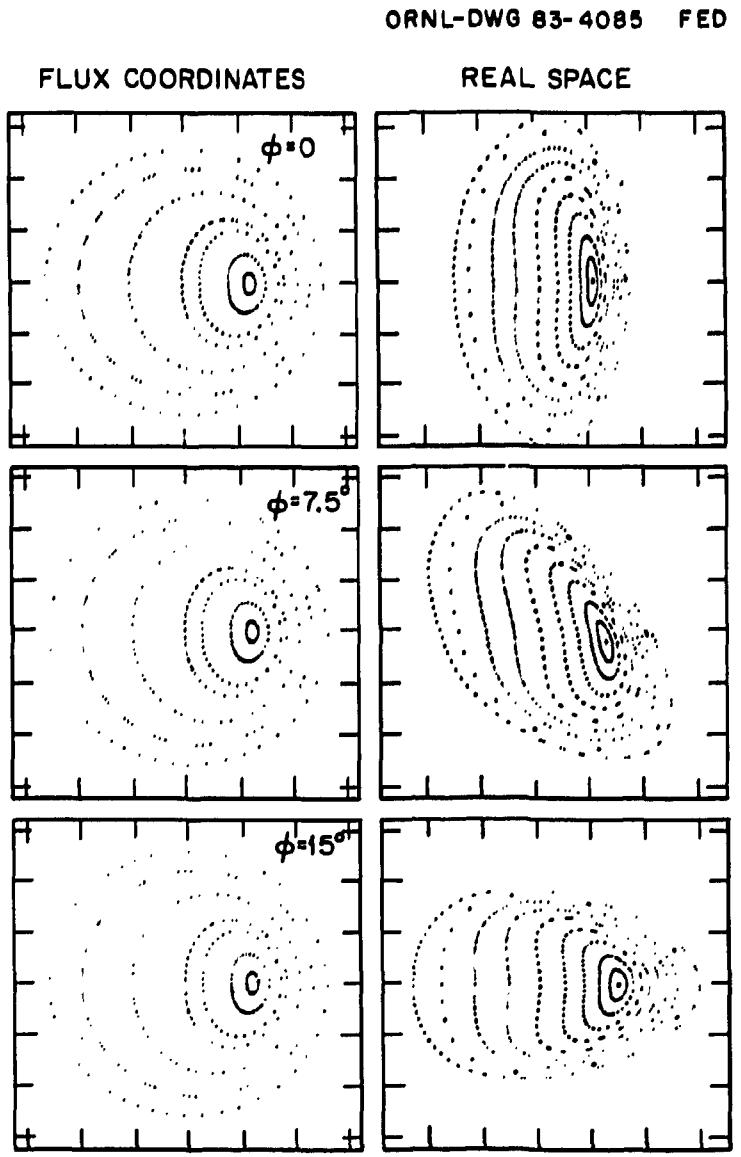

Fig. 1. Comparison of equilibrium flux surfaces in $(\rho_v, \theta_v, \phi_v)$ space and real space for planar axis ATF (β_0 = 5%).

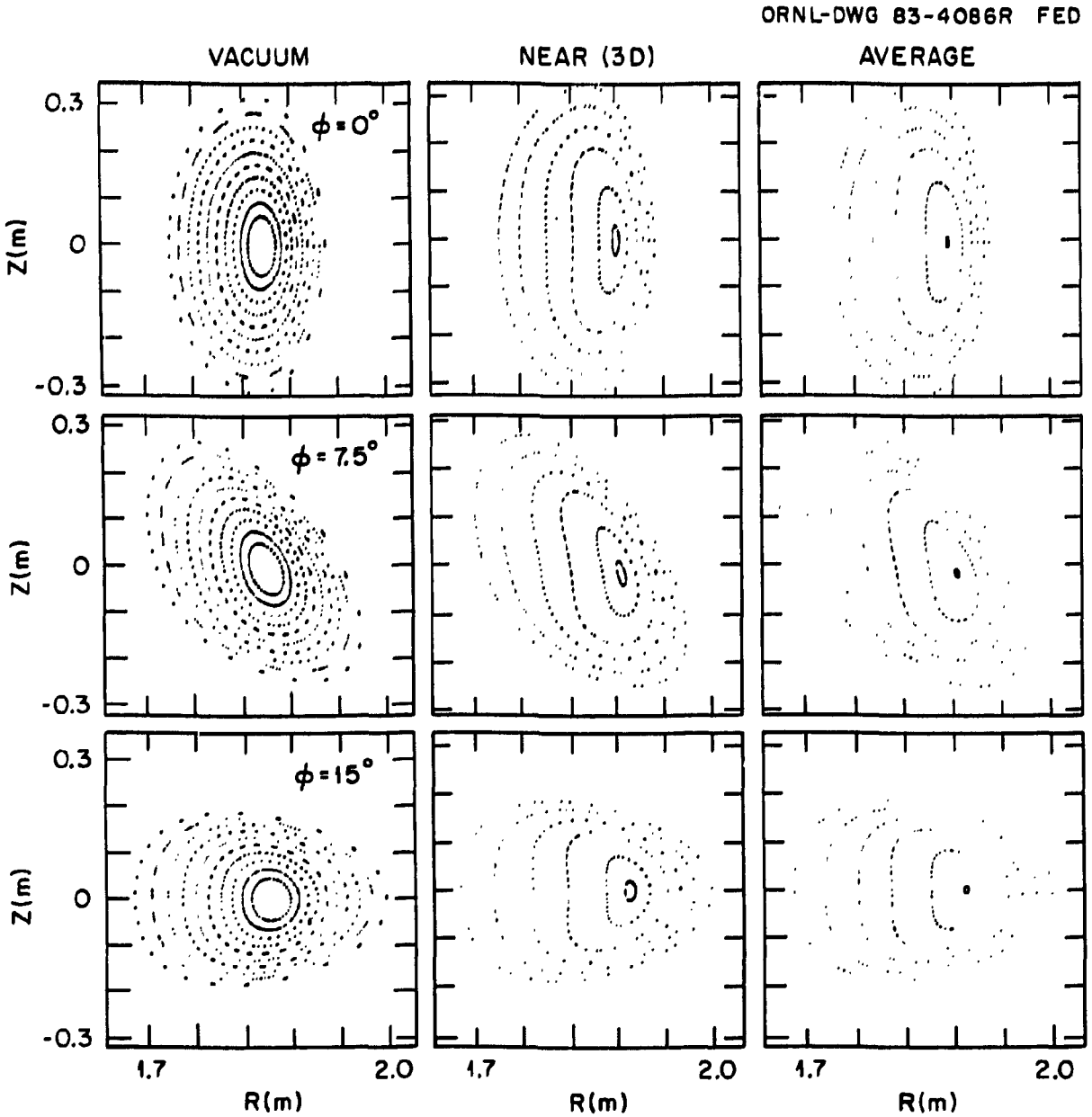

Fig. 2. Comparison between equilibrium flux surfaces computed with NEAR (3-D) and average method ($\beta_0 = 5\%$, $\langle P \rangle \propto \psi^2$) for planar axis ATF. Vacuum flux surfaces are shown for comparison.

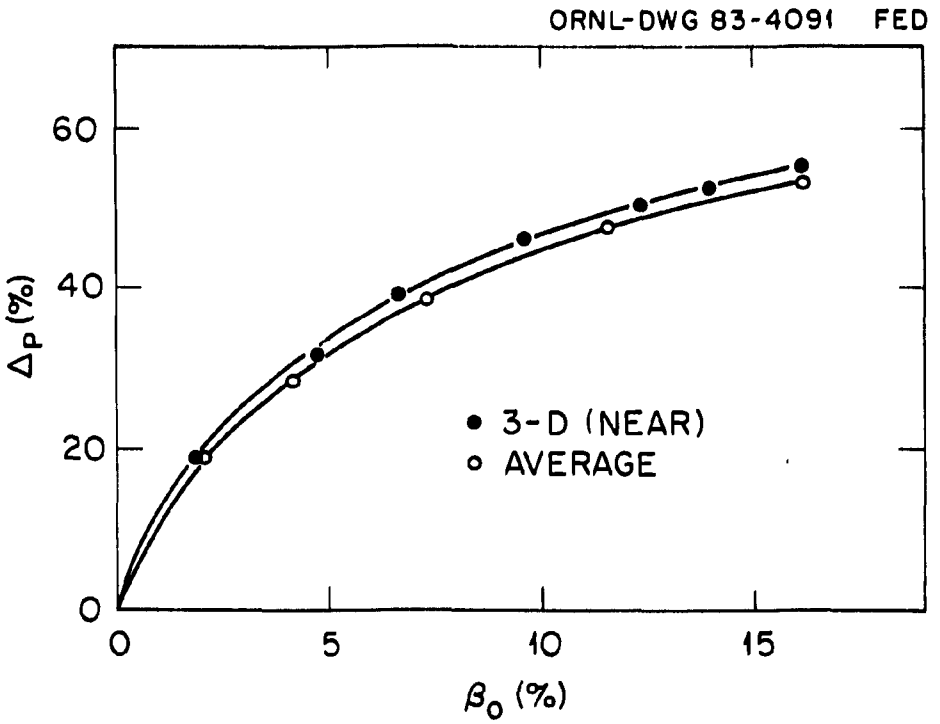

Fig. 3. Shift (Δ_p) as a function of β_0 for the planar axis ATF.

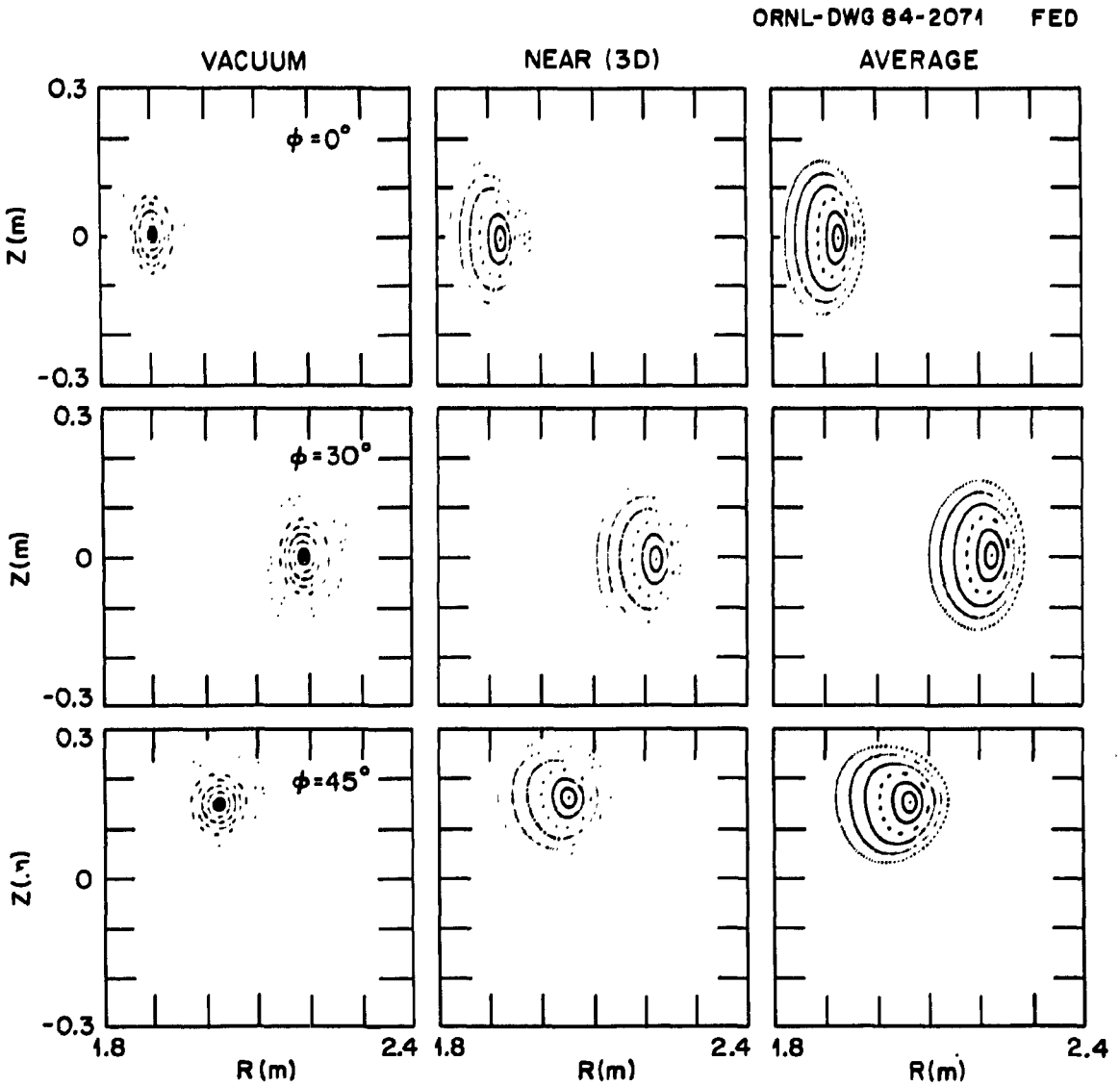

Fig. 4. Comparison between equilibrium flux surfaces computed with NEAR (3-D) and average method ($\beta_0 = 2.6\%$, $\langle P \rangle \propto \psi^2$) for helical axis ATF. Vacuum flux surfaces are also shown for comparison.

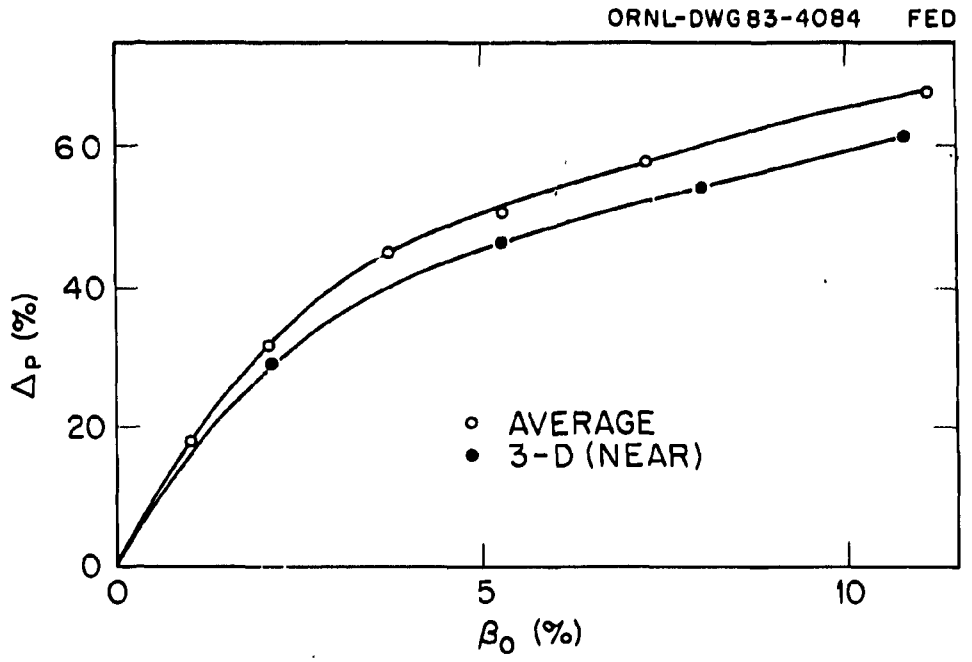

Fig. 5. Shift, (Δ_p) as a function of β_0 for the helical axis ATF.

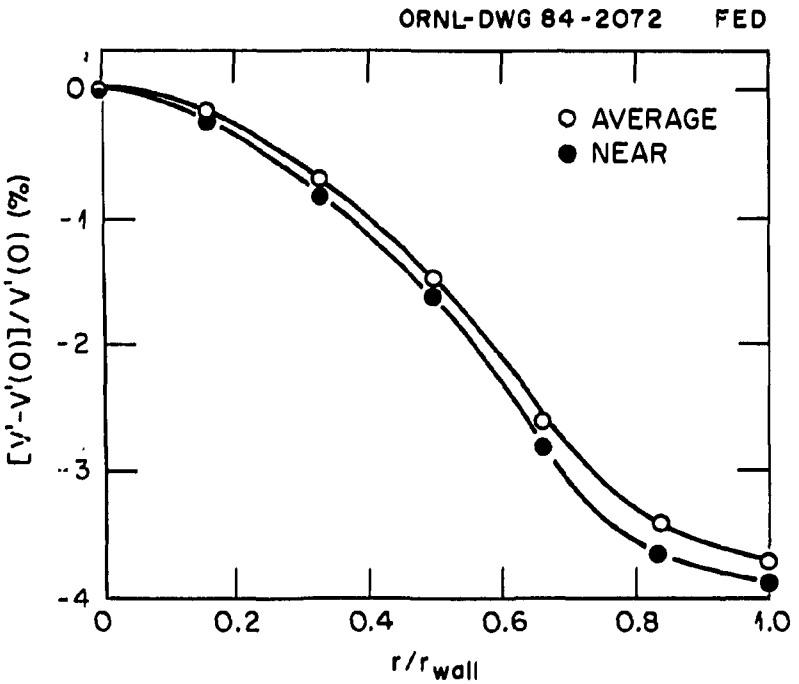

Fig. 6. Comparison of V′ profile for helical axis ATF, between 3-D and average method calculations. Parameters are the same as in Fig. 4.

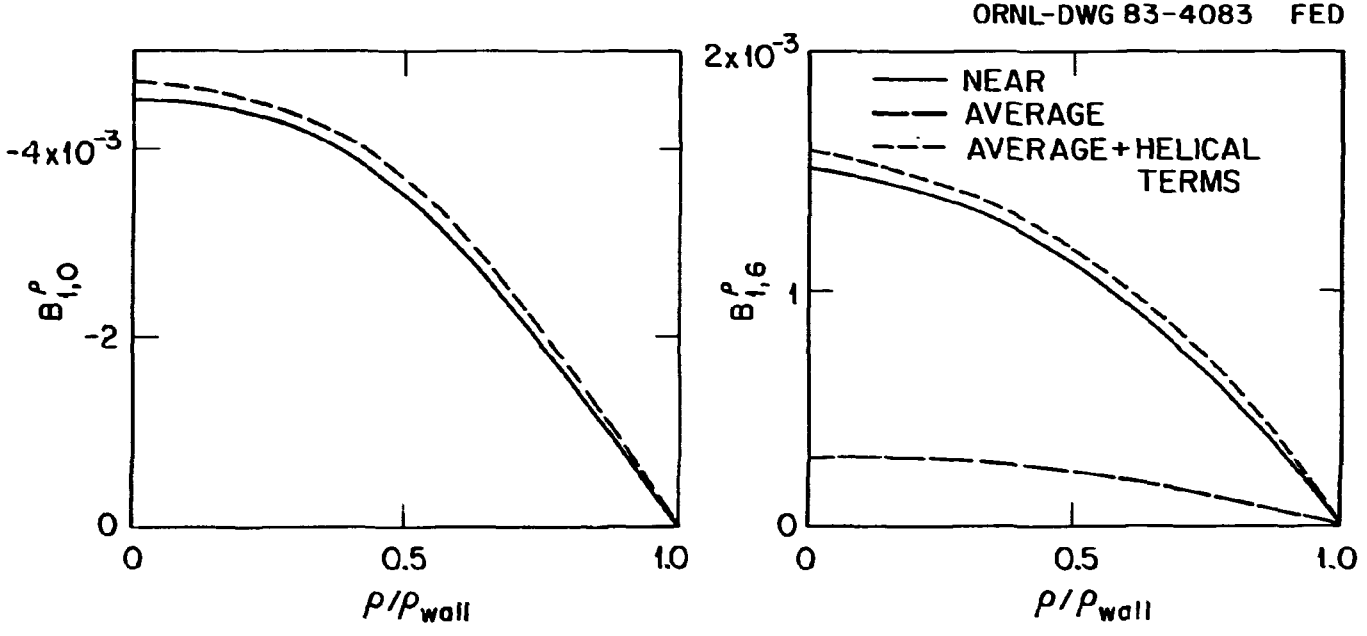

Fig. 7. Comparison of radial structure of B^{ρ} harmonics computed with the 3-D NEAR code and as corrections to average method equilibria by solving Eq. (32), for helical axis ATF ($\beta_0 = 2\%$, $\langle P \rangle \propto \psi^2$). Dominant toroidal (1,0) and helical harmonic (1,6) are shown.

ACKNOWLEDGMENT

We should like to thank J. L. Johnson for several useful discussions.

ORNL/TM-9147
Dist. Category UC-20 g

INTERNAL DISTRIBUTION

1-5. B. A. Carreras
6. R. A. Dory
7. J. Dunlap
8. L. Garcia
9. J. H. Harris
10-15. T. C. Hender
16. H. R. Hicks
17. J. A. Holmes
18. V. E. Lynch
19. Y-K. M. Peng
20. J. Sheffield
21. D. Sigmar
22-23. Laboratory Records Department
24. Laboratory Records, ORNL-RC
25. Document Reference Section
26. Central Research Library
27. Fusion Energy Division Library
28. Fusion Energy Division Publications Office
29. ORNL Patent Office

EXTERNAL DISTRIBUTION

30. A. Boozer, Princeton Plasma Physics Laboratory, P.O. Box 451, Princeton, NJ 08544
31. A. Reiman, Princeton Plasma Physics Laboratory, P.O. Box 451, Princeton, NJ 08544
32. J. Johnson, Princeton Plasma Physics Laboratory, P.O. Box 451, Princeton, NJ 08544
33. J. Cary, Institute for Fusion Studies, University of Texas, Austin, TX 78712
34. H. Berk, Institute for Fusion Studies, University of Texas, Austin, TX 78712
35. N. Hitchon, Department of Nuclear Engineering, University of Wisconsin, Madison, WI 53706
36. Office of the Assistant Manager for Energy Research and Development, Department of Energy, Oak Ridge Operations, Box E, Oak Ridge, TN 37830
37. J. D. Callen, Department of Nuclear Engineering, University of Wisconsin, Madison, WI 53706
38. R. W. Conn, Department of Chemical, Nuclear, and Thermal Engineering, University of California, Los Angeles, CA 90024
39. S. O. Dean, Director, Fusion Energy Development, Science Applications, Inc., 2 Professional Drive, Gaithersburg, MD 20760
40. H. K. Forsen, Bechtel Group, Inc., Research Engineering, P.O. Box 3965, San Francisco, CA 94105
41. R. W. Gould, Department of Applied Physics, California Institute of Technology, Pasadena, CA 91125
42. D. G. McAlees, Exxon Nuclear Company, Inc., 777 106th Avenue, NE, Bellevue, WA 98009
43. P. J. Reardon, Princeton Plasma Physics Laboratory, P.O. Box 451, Princeton, NJ 08544
44. W. M. Stacey, Jr., School of Nuclear Engineering, Georgia Institute of Technology, Atlanta, GA 30332

45. G. A. Eliseev, I. V. Kurchatov Institute of Atomic Energy, P.O. Box 3402, 123182 Moscow, U.S.S.R.
46. V. A. Glukhikh, Scientific-Research Institute of Electro-Physical Apparatus, 188631 Leningrad, U.S.S.R.
47. I. Spighel, Lebedev Physical Institute, Leninsky Prospect 53, 117924 Moscow, U.S.S.R.
48. D. D. Ryutov, Institute of Nuclear Physics, Siberian Branch of the Academy of Sciences of the U.S.S.R., Sovetskaya St. 5, 630090 Novosibirsk, U.S.S.R.
49. V. T. Tolok, Kharkov Physical-Technical Institute, Academical St. 1, 310108 Kharkov, U.S.S.R.
50. R. Varma, Physical Research Laboratory, Navrangpura, Ahmedabad, India
51. Bibliothek, Max-Planck-Institut fur Plasmaphysik, D-8046 Garching bei Munchen, Federal Republic of Germany
52. Bibliothek, Institut fur Plasmaphysik, KFA, Postfach 1913, D-5170 Julich, Federal Republic of Germany
53. Bibliotheque, Centre de Recherches en Physique des Plasmas, 21 Avenue des Bains, 1007 Lausanne, Switzerland
54. Bibliotheque, Service du Confinement des Plasmas, CEA, B.P. 6, 92 Fontenay-aux-Roses (Seine), France
55. Documentation S.I.G.N., Departement de la Physique du Plasma et de la Fusion Controlee, Centre d'Etudes Nucleaires, B.P. No. 85, Centre du Tri, 38041 Cedex, Grenoble, France
56. Library, Culham Laboratory, UKAEA, Abingdon, Oxfordshire, OX14 3DB, England
57. Library, Institute of Physics, Academia Sinica, Beijing, Peoples Republic of China
58. Library, Institute of Plasma Physics, Nagoya University, Nagoya 64, Japan
59. Library, International Centre for Theoretical Physics, Trieste, Italy
60. Library, Laboratorio Gas Ionizzati, Frascati, Italy
61. Library, Plasma Physics Laboratory, Kyoto University, Gokasho Uji, Kyoto, Japan
62. Plasma Research Laboratory, Australian National University, P.O. Box 4, Canberra, A.C.T. 2000, Australia
63. Thermonuclear Library, Japan Atomic Energy Research Institute, Tokai, Naka, Ibaraki, Japan
64. J. F. Clarke, Associate Director for Fusion Energy, Office of Fusion Energy, Office of Energy Research, Mail Stop G-256, U.S. Department of Energy, Washington, DC 20545
65. D. B. Nelson, Acting Director, Division of Applied Plasma Physics, Office of Fusion Energy, Office of Energy Research, Mail Stop G-256, U.S. Department of Energy, Washington, DC 20545
66. M. N. Rosenbluth, RLM 11.218, Institute for Fusion Studies, University of Texas, Austin, TX 78712
67. W. Sadowski, Fusion Theory and Computer Services Branch, Office of Fusion Energy, Office of Energy Research, Mail Stop G-256, U.S. Department of Energy, Washington, DC 20545

68. N. A. Davies, Tokamak Systems Branch, Office of Fusion Energy, Office of Energy Research, Mail Stop G-256, U.S. Department of Energy, Washington, DC 20545
69. E. Oktay, Tokamak Systems Branch, Office of Fusion Energy, Office of Energy Research, Mail Stop G-256, U.S. Department of Energy, Washington, DC 20545
70. Theory Department Read File, c/o D. W. Ross, Institute for Fusion Studies, University of Texas at Austin, Austin, TX 78712
71. Theory Department Read File, c/o R. C. Davison, Director, Plasma Fusion Center, 167 Albany Street, Cambridge, MA 02139
72. Theory Department Read File, c/o F. W. Perkins, Princeton Plasma Physics Laboratory, P.O. Box 451, Princeton, NJ 08544
73. Theory Department Read File, c/o L. Kovrizhnykh, Lebedev Institute of Physics, Academy of Sciences, 53 Leninsky Prospect, Moscow, U.S.S.R. V312
74. Theory Department Read File, c/o B. B. Kadomtsev, I. V. Kurchatov Institute of Atomic Energy, P.O. Box 3402, Moscow, U.S.S.R. 123182
75. Theory Department Read File, c/o T. Kamimura, Institute of Plasma Physics, Nagoya University, Nagoya, Japan
76. Theory Department Read File, c/o C. Mercier, Euratom-CEA, Service de Recherches sur la Fusion Controlee, Fontenay-aux-Roses (Seine), France
77. Theory Department Read File, c/o T. E. Stringer, JET Joint Undertaking, Culham Laboratory, Abingdon, Oxfordshire, OX14 3DB, England
78. Theory Department Read File, c/o K. Roberts, Culham Laboratory, Abingdon, Oxon, OX14 3DB, England
79. Theory Department Read File, c/o D. Biskamp, Max-Planck-Institut fur Plasmaphysik, D-8046 Garching bei Munchen, Federal Republic of Germany
80. Theory Department Read File, c/o T. Takeda, Japan Atomic Energy Research Institute, Tokai, Naka, Ibaraki, Japan
81. Theory Department Read File, c/o C. S. Liu, GA Technologies, Inc., P.O. Box 81608, San Diego, CA 92138
82. Theory Department Read File, c/o L. D. Pearlstein, Lawrence Livermore National Laboratory, P.O. Box 808, Livermore, CA 94550
83. Theory Department Read File, c/o R. Gerwin, CTR Division, MS 640, Los Alamos National Laboratory, P.O. Box 1663, Los Alamos, NM 87545 87545
84. Library, FOM Instituut voor Plasma-Fysica, Rijnhuizen, Jutphaas, The Netherlands
85. J. F. Decker, Director, Division of Applied Plasma Physics, Office of Fusion Energy, Office of Energy Research, Mail Stop G-256, U.S. Department of Energy, Washington, DC 20545

86-244. Given distribution as shown in TID-4500 Magnetic Fusion Energy (Category Distribution UC-20 g: Theoretical Plasma Physics)